THE JOURNAL OF BIOLOGICAL CHEMISTRY
Vol. 280, No. 11, Issue of March 18, pp. 10855–10860, 2005

Printed in U.S.A.

ATP-dependent and ATP-independent Roles for the Rad54 Chromatin Remodeling Enzyme during Recombinational Repair of a DNA Double Strand Break*

Received for publication, December 21, 2004, and in revised form, January 12, 2005
Published, JBC Papers in Press, January 14, 2005, DOI 10.1074/jbc.M414388200

Branden Wolner and Craig L. Peterson‡

From the Program in Molecular Medicine, University of Massachusetts Medical School, Worcester, Massachusetts 01605

The efficient and accurate repair of DNA double strand breaks (DSBs) is critical to cell survival, and defects in this process can lead to genome instability and cancers. In eukaryotes, the Rad52 group of proteins dictates the repair of DSBs by the error-free process of homologous recombination (HR). A critical step in eukaryotic HR is the formation of the initial Rad51-single-stranded DNA presynaptic nucleoprotein filament. This presynaptic filament participates in a homology search process that leads to the formation of a DNA joint molecule and recombinational repair of the DSB. Recently, we showed that the Rad54 protein functions as a mediator of Rad51 binding to single-stranded DNA, and here, we find that this activity does not require ATP hydrolysis. We also identify a novel Rad54-dependent chromatin remodeling event that occurs *in vivo* during the DNA strand invasion step of HR. This ATP-dependent remodeling activity of Rad54 appears to control subsequent steps in the HR process.

Double strand breaks (DSBs)[1] are a common form of DNA damage, resulting from a variety of environmental insults including ionizing radiation and chemical attack. The most common cause of DSBs is internal reactive oxygen species, accounting for thousands of breaks per cell per day. The inability to repair these breaks leads to genomic instability. Misrepair of these breaks can result in deletions, insertions, and translocations. In higher eukaryotes, improper DSB repair can lead to tumorigenesis. It is therefore of vital importance that cells repair these breaks accurately and faithfully.

Several pathways have evolved for the repair of DSBs. In yeast, the predominant pathway is thought to be homologous recombination (1, 2). Homologous recombination (HR) provides an "error-free" method for repairing DSBs as it utilizes homologous DNA sequences as a template to repair the lesion with no loss of genetic information. The genes in the *RAD52* epistasis group, required for HR, are highly conserved from yeast to man (2–4), highlighting the importance of this molecular pathway.

Studies in yeast have suggested a sequence of molecular events that occur following the formation of a DSB (2, 4, 5). Nucleolytic end processing leads to resection of the 5′ ends of DNA that flank the break, generating long stretches of 3′ single-stranded DNA. Rad51p binds the single-stranded DNA, forming right-handed helical nucleoprotein filaments. *In vitro*, Rad52p (6), Rad54p (7), and a Rad55p/Rad57p heterodimer (8) mediate this early step by overcoming the inhibitory effects of the heterotrimeric single-stranded DNA-binding protein, RPA. *In vivo*, these same Rad proteins are also required for optimal recruitment of Rad51p to DNA surrounding a single DSB in yeast (7, 9). The Rad51-nucleoprotein filament is believed to search the genome for homologous sequences, resulting in the formation of a heteroduplex "joint molecule" (10). Joint molecule formation is followed by extension of the incoming strand by DNA polymerases and branch migration. The end result is the repair of the DSB without loss of genetic information (2).

Rad54p is a member of the Swi2/Snf2 family of DNA-stimulated ATPases (11), and like Swi2/Snf2, Rad54p shows ATP-dependent chromatin remodeling activity *in vitro* (12–14). Rad54p also binds to both single-stranded DNA (7) and Rad51p (15–17), and these latter two activities are believed to play key roles in the stimulation of Rad51-single-stranded DNA nucleoprotein filament formation. *In vitro*, this mediator activity of Rad54 is optimal at substoichiometric ratios of Rad54p to Rad51p (7), although in other types of *in vitro* assays, Rad54p functions best at stoichiometric levels (18–20). These *in vitro* studies raise the question of whether Rad54p might be a stoichiometric component of the extended Rad51 nucleoprotein filament *in vivo*.

In vitro, the ATPase activity of Rad54 is required to promote homologous DNA pairing between a Rad51-nucleoprotein filament and a double-stranded DNA or chromatin donor (12, 21). In addition, yeast harboring mutant alleles of *RAD54* that disrupt the ATPase domain exhibit sensitivity to DNA-damaging agents (15) and defects in intrachromosomal recombination (21). In contrast, the ATPase-defective *RAD54* alleles have little effect on interchromosomal recombination. This suggests that Rad54p may have several functions *in vivo* and that some, but not all, require a functioning ATPase domain. In this study, we use chromatin immunoprecipitation (ChIP) to assess the composition of the presynaptic nucleoprotein filament *in vivo* and to investigate the role of the Rad54 ATPase activity. We find that the ATPase activity of Rad54 is dispensable for early steps in HR but, in contrast, the ATPase activity of Rad54 is required for a chromatin remodeling step that occurs during strand invasion.

MATERIALS AND METHODS

Plasmids and Strains—The 2-μm plasmid containing the *RAD54* gene plus 400 bp of upstream genomic DNA was a kind gift of Hannah Klein (New York University). A 3.2-kb NotI-SalI fragment containing the *RAD54* genomic sequences was excised and cloned into the NotI-

* This work was supported by Grants GM64233 (to B. W.) and GM54096 (to C. L. P.) from the National Institutes of Health. The costs of publication of this article were defrayed in part by the payment of page charges. This article must therefore be hereby marked "*advertisement*" in accordance with 18 U.S.C. Section 1734 solely to indicate this fact.

‡ To whom correspondence should be addressed: Program in Molecular Medicine, University of Massachusetts Medical School, 373 Plantation St., Biotech 2, Ste. 203, Worcester, MA, 01605. Tel.: 508-856-5858; Fax: 508-856-5011; E-mail: craig.Peterson@umassmed.edu.

[1] The abbreviations used are: DSB, double strand breaks; IP, immunoprecipitation; ChIP, chromatin IP; MNase, micrococcal nuclease; SIE, strand invasion/extension.

SalI sites in pRS406. The codon for lysine 341 was mutagenized to arginine by QuikChange mutagenesis (Stratagene). The site-specific mutation was verified by sequencing. The mutant and wild-type plasmids were linearized with NcoI and transformed into *rad54*Δ strains that either contained (CY1166) or lacked (CY916) silent mating type loci. All other strains used here were described previously (7).

Chromatin Immunoprecipitation—Polyclonal Rad51 and Rad52 antibodies were obtained from Santa Cruz Biotechnology. For ChIP against Rad54p and Rad55p, the proteins were tagged at their carboxyl termini with 13 copies of the c-Myc epitope as described previously (7) and immunoprecipitated with monoclonal anti-Myc (9E10) antibody (Santa Cruz Biotechnology).

ChIP assays were performed as described previously (7) with modification as follows. After adsorption to protein A-Sepharose, cross-linked antigens were eluted in 250 μl of 2× proteinase K buffer (2× proteinase K buffer is 20 mM Tris-Cl, pH = 8.0, 10 mM EDTA, 1% SDS) by shaking at 65 °C for 10 min. Beads were pelleted by pulse centrifugation, and the supernatants were diluted with an equal volume of water. Proteinase K (100 mg) was added, and samples were incubated at 42 °C for 1 h followed by 65 °C overnight. Lithium chloride (400 mM final) was added, and samples were extracted once with phenol:chloroform:iso-amyl alcohol (25:24:1) and once with chloroform:iso-amyl alcohol (24:1). Samples were then precipitated with 20 μg of glycogen and 1 ml of 100% ethanol.

Radioactive semiquantitative PCR was performed and analyzed as described previously (7). Multiplex PCR reactions containing only the break-proximal (18 bp) and break-distal (900 bp) primers (see Fig. 1*a*) failed to amplify the expected 882-bp product even when the extension times were increased to 2 min (not shown), indicating that the DNA from the two *MAT* regions immunoprecipitate independently.

Micrococcal Nuclease and Southern Blotting—For micrococcal nuclease (MNase) assays, 50-ml cultures were grown in YEP + raffinose to mid-log phase and induced with galactose as described above for ChIP assays. Parallel uninduced cultures served as negative controls. Cultures were cross-linked with formaldehyde, and extracts were prepared as for ChIP. Extracts were not sonicated but were instead treated with various amounts of MNase for 15 min at 37 °C. For optimal MNase digestion, magnesium chloride (20 mM final) and calcium chloride (2 mM final) were added to the extracts. Each 50-ml culture represented one MNase digestion reaction. These reactions were quenched with 1% SDS and 5 mM EDTA and then treated with 500 mg of proteinase K at 42° for 2 h and then at 65° for 5 h to reverse the cross-links. DNA was extracted twice with phenol:chloroform:iso-amyl alcohol (25:24:1) and once with chloroform:iso-amyl alcohol (24:1) and then precipitated with sodium acetate and ethanol. Dried DNA was dissolved in 400 μl of 10 mM Tris, pH 7.4/1 mM EDTA with 300 mg RNase-A, incubated at 37° for 1 h, extracted once with phenol:chloroform:iso-amyl alcohol and once with chloroform:iso-amyl alcohol, and then precipitated again with sodium acetate and ethanol. DNA was dissolved in water and digested with HindIII (New England Biolabs) in the appropriate buffer overnight at 37 °C. After precipitation, DNA was dissolved in 20 μl of water and electrophoresed on 1.3% agarose, 1× Tris-borate-EDTA gels. Southern blotting was carried out as described (22). The probe was made by PCR with genomic DNA as a template and primers (5′ to 3′): GCAAAGCTTACTTCATTTATTAG and CTTATTGTGCTTTGTTGGGTG. The location of this probe is illustrated below (see Fig. 5*a*). The PCR product was gel-purified (Qiagen) and labeled by the random primer method (Roche Applied Science).

For analysis of HO cleavage at *HML*, 25-ml cultures were grown in YEP + raffinose and induced as described above. Formaldehyde fixation was omitted. Cells were harvested by centrifugation, washed with water, transferred to microcentrifuge tubes, and suspended in 200 μl of genomic DNA buffer (2% Triton X-100, 1% SDS, 100 mM sodium chloride, 10 mM Tris-Cl, pH = 8.0, 1 mM EDTA) and 200 μl of phenol:chloroform:iso-amyl alcohol (25:24:1) with 250 μl of zirconium beads (Biospec Products). Cells were lysed by shaking on a multivortexer for 10 min after which 200 μl of TE was added. Samples were centrifuged for 5 min, and the aqueous phase was extracted with chloroform:iso-amyl alcohol. DNA was treated with 30 mg of RNase-A for 5 min at 37° and then precipitated with sodium acetate and ethanol. Dried DNA was dissolved in water and digested overnight with either HindIII or BamHI (NEB). The DNA was precipitated, and Southern blotting was performed as described above.

RESULTS

Previously, we used chromatin immunoprecipitation analyses to monitor the recruitment of Rad proteins to a single, HO-induced DSB at the yeast *MAT* locus (7). Although our studies focused on recruitment events immediately proximal to the DSB, Haber and colleagues (9) demonstrated that Rad51p is cross-linked over several kilobases of DNA surrounding the DSB in yeast. To determine whether Rad54p and the other members of the *RAD52* group are part of this extended nucleoprotein filament, chromatin immunoprecipitation analyses were performed for Rad51p, Rad52p, Rad54p, and Rad55p using DNA primer sets that monitor recruitment events both proximal to (18–257 bp) and distal from (600–900 bp) an HO-induced DSB (Fig. 1*a*). We also included primers to the *PHO5* locus as a control in the multiplex PCR analysis. Consistent with previous studies (7, 9), we observe rapid recruitment of Rad51p to DNA both proximal to and distal from the induced DSB (Fig. 1, *b* and *c*). Likewise, we find that Rad52p and Rad55p are also recruited to both regions, consistent with their association with the entire Rad51p nucleoprotein filament (Fig. 1, *b* and *c*). In contrast, Rad54p is only cross-linked to DNA proximal to the DSB (Fig. 1, *b* and *c*). Identical results are found in ChIP time courses that are extended to 8 h (data not shown). Thus, these data indicate that Rad54p is not a stoichiometric component of a Rad51-nucleoprotein filament *in vivo*, and furthermore, the data indicate that Rad54p may only associate with the 3′ end of the presynaptic complex.

Previously, we showed that Rad52p, Rad55p, and Rad54p are all mediators of Rad51p recruitment to DNA proximal to an HO-induced DSB *in vivo* (7). Given that Rad54p is only associated with this same proximal region, we tested whether the mediator activity of Rad54 is restricted to the 3′ end of the presynaptic filament. As we showed previously, deletion of *RAD54* causes a 6-fold decrease in recruitment of Rad51p to DNA proximal to the HO-induced DSB (Fig. 2, *a* and *b*). However, cross-linking of Rad51p at the distal region (600–900 bp) is reduced less than 2-fold in the *rad54* deletion strain. Likewise, binding of Rad51p to a medial region (250–535 bp, Fig. 2*b*) is reduced only 3-fold in the absence of Rad54p. In contrast, deletion of the *RAD52* gene leads to a complete absence of Rad51p recruitment throughout the entire region tested (Fig. 2*b*). Thus, these data distinguish the mediator activities of Rad54p and Rad52p, and they indicate that the Rad54p mediator activity is most crucial in the same region where Rad54p itself binds, at the extreme 3′ end of the presynaptic filament.

Based on analogy to prokaryotic homologous recombination (4), the Rad51p presynaptic filament is believed to search for homologous sequences until it is able to form an unstable paranemic joint in which homologous sequences are aligned, but the DNA strands are not topologically intertwined. This unstable joint is subsequently extended to the 3′ end of the Rad51p filament, forming a stable plectonemic DNA joint. Previously, we showed that *RAD54* is required for cross-linking of Rad51p to homologous donor sequences, and at that time, we concluded that Rad54p might play a role in the homology search process (7). However, this analysis only monitored binding of Rad51p to donor sequences that are homologous to the extreme 3′ end of the incoming presynaptic filament (Fig. 3; *HML* proximal), a region that we have now shown is devoid of Rad51p in a *rad54* deletion strain. Thus, it is possible that an unstable paranemic joint might be formed in the absence of *RAD54*, given the high levels of Rad51p that are bound to the distal end of the presynaptic filament.

Fig. 3*b* shows a representative Rad51p ChIP analysis in strains harboring a galactose-inducible *HO* gene that also contain the homologous donor sequences, *HML* and HMR. PCR analysis of Rad51p immunoprecipitates included primer sets for the *PHO5* control locus, the *MAT* locus, and the *HML* homologous donor locus. For *HML*, two sets of primer pairs

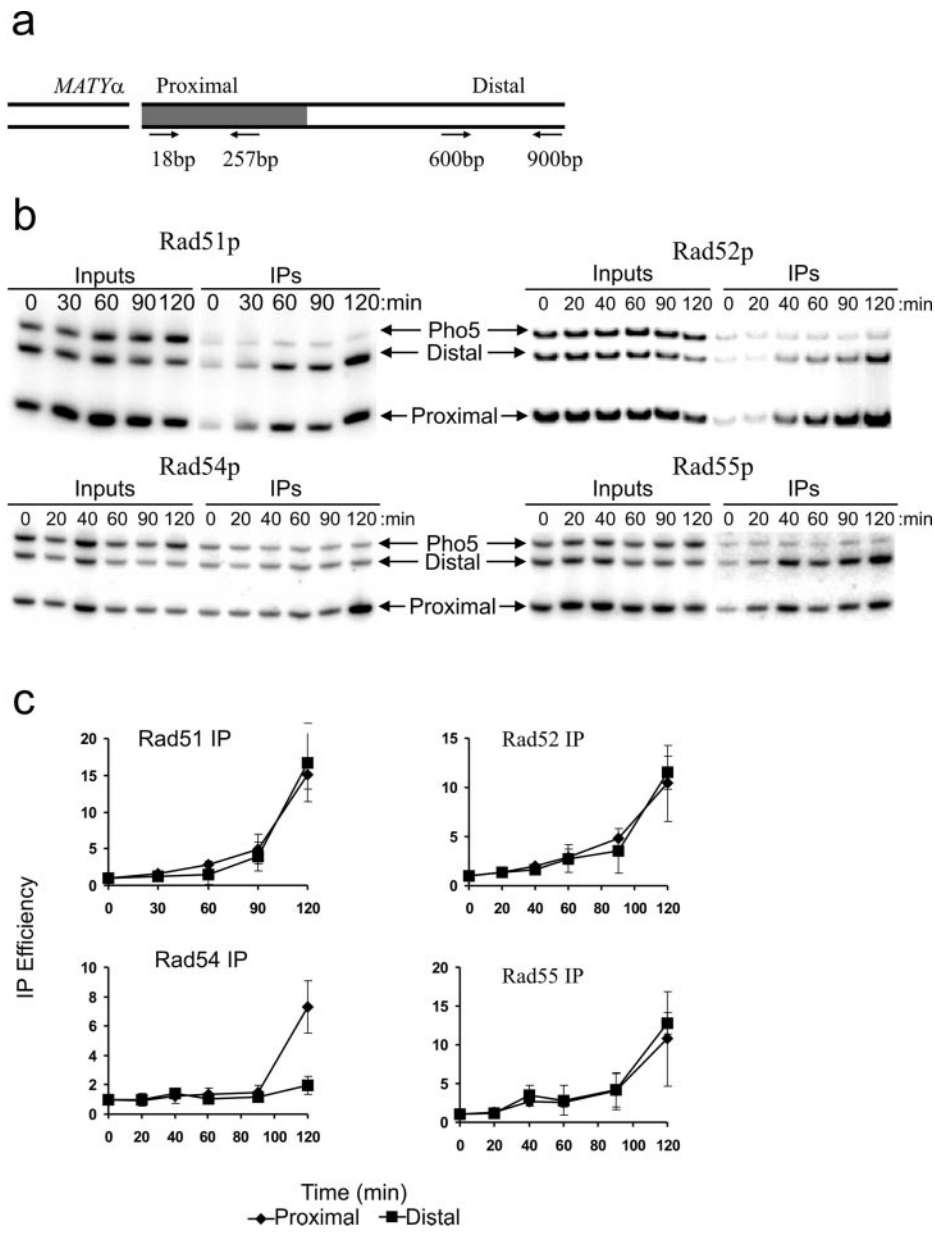

FIG. 1. **Composition of nucleoprotein filament.** *a*, schematic diagram of the *MAT* locus in donorless strains. *Arrows* indicate the positions of the primers used in PCR. The *shaded area* indicates the region of extended homology between *MAT* and *HMLα*. *b*, representative ChIP assays. Donorless strains were induced with galactose for the indicated times. "Input" DNA represents 1% of the amount of DNA used for immunoprecipitation. Primers to the *PHO5* promoter region on chromosome 2 were included as controls. *c*, data from several ChIP assays were quantitated using ImageQuant software (Amersham Biosciences) and plotted in the graphs on the *right*. The IP efficiency represents the -fold increase in the percent immunoprecipitated DNA (*i.e.* IP/Input) *versus* the control locus and normalized to time zero. Each chart represents the average of 3–5 experiments each.

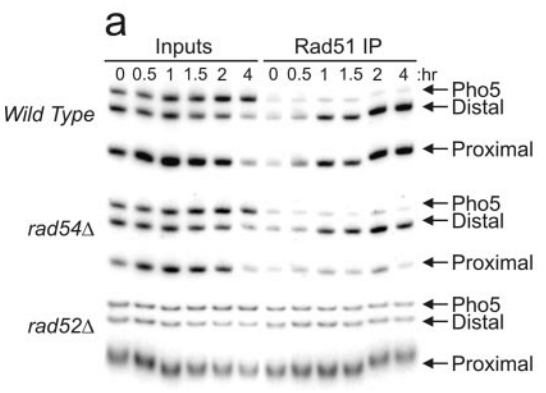

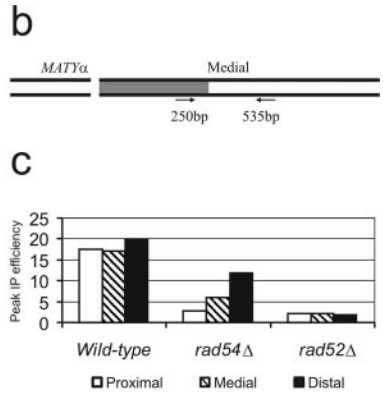

FIG. 2. **Rad54p mediator activity is required in the break-proximal region.** *a*, representative ChIP assays against Rad51p in wild-type, *rad54*Δ, and *rad52*Δ strains. The PCR product bands are as indicated in the legend for Fig. 1*b*. *b*, schematic indicating the locations of the *MAT-Z* medial region primers. *c*, summary of data for mediator activities of Rad54 and Rad52. Peak IP efficiency represents the highest IP efficiency seen for each region in each strain. IP efficiency was determined as described in the legend for Fig. 1.

were used: 1) a proximal *HML* set that detects synapsis of the 3′ end of the incoming filament and 2) a distal *HML* set that detects synapsis of the medial region of the presynaptic filament (Figs. 2*b* and 3*a*). As we observed previously (7), Rad51p is detected at the *MAT* locus (Fig. 3*b*) and at the proximal *HML* donor site in the wild-type strain (not shown). However, detection of Rad51p in the distal region of *HML* was not observed even in the wild-type strain unless we dramatically decreased the amount of sonication during the ChIP procedure (Fig. 3, *b* and *c*). Importantly, decreasing the extent of sonication had little impact on the immunoprecipitation efficiency of *MAT* sequences in the wild-type strain. In the *rad54* deletion strain, Rad51p was not detectable at the proximal *HML* region (not shown), confirming our previous results (7). However, Rad51p

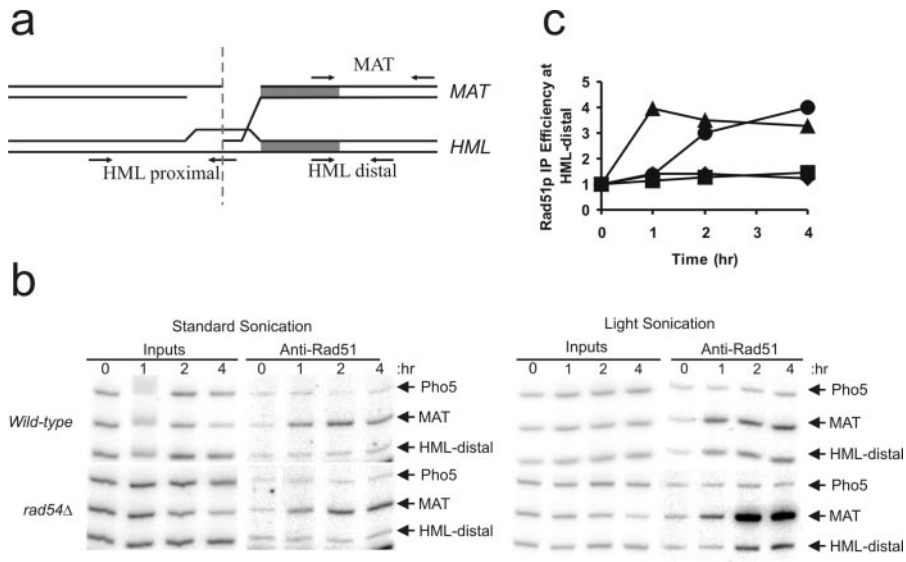

FIG. 3. **Unstable recombination joints form downstream in the absence of RAD54.** *a*, schematic diagram of a plectonemic recombination joint between the HO-cleaved *MAT* locus aligned with the homologous *HML* region. Primers for amplicons are indicated. The *vertical dashed bar* indicates the HO recognition sites. *b*, representative ChIP assays demonstrating that Rad51p crosslinking to the distal *HML* region is sensitive to sonication treatment. Standard sonication is five rounds of six pulses (2 s/pulse). Light sonication is reduced to only two rounds of six pulses. *c*, data for *HML*-distal in *panel b* were quantitated as described under "Materials and Methods." Wild type, standard sonication (*diamonds*); *rad54*Δ, standard sonication (*squares*); wild type, light sonication (*triangles*); *rad54*Δ, light sonication (*circles*).

was seen bound to the downstream *HML* region in the *rad54* deletion strain when sonication cycles were decreased (Fig. 3, *b* and *c*). Thus, these data indicate that *RAD54* is not required for a successful homology search, but rather, that the absence of Rad54p leads to the formation of an unstable DNA joint that may only be paranemic in nature. A similar conclusion has been made by Sugawara *et al.* (9).

Rad54 is unique among those proteins known to mediate the binding of Rad51p to single-stranded DNA as Rad54 is a potent DNA-stimulated ATPase. Several roles have been proposed for the ATPase activity of Rad54, including ATP-dependent DNA duplex separation during strand invasion (19, 21, 23), ATP-dependent removal of Rad51p at a post-synapsis step (24), as well as ATP-dependent chromatin remodeling during the homology search or DNA strand invasion (12, 25). To identify ATP-dependent role(s) for Rad54p during HR, we created isogenic yeast strains that express wild-type Rad54p or an ATPase-defective version of Rad54, rad54K341R. Similar to previous studies (1, 15), both the *rad54* deletion strain and the strain that expresses the ATPase-defective version, rad54K341R, are hypersensitive to the DNA-damaging agent, methyl methanesulfonate (data not shown).

ChIP analyses were performed to monitor Rad51p recruitment in the isogenic *RAD54*, *rad54K341R*, and *rad54* deletion strains. In the isogenic strain set that lacks homologous donors, Rad51p was detected at both the *MAT* proximal and the *MAT* distal regions in the *RAD54* strain, but binding was only detected at the distal region in the *rad54* deletion strain (Fig. 4*a*). When the rad54K341R allele was expressed, Rad51p recruitment to the proximal region was restored. Thus, this role for Rad54p in facilitating Rad51p recruitment does not require an intact ATPase domain. Furthermore, in a similar isogenic strain set that harbors homologous donors, both Rad54p and Rad54K341R supported binding of Rad51p to the *HML* proximal region, even under normal sonication conditions (Fig. 4*b*). Thus, the ATPase-defective version of Rad54p is able to rescue full synapsis at the *HML* donor. However, only strains harboring wild-type Rad54p were able to extend the DNA joint and generate a strand invasion/extension (SIE) product (Fig. 4*c*). These data demonstrate that Rad54p has at least two functions during recombinational DNA repair: 1) a presynaptic activity that helps recruit Rad51p to single-stranded DNA and is independent of ATP hydrolysis and 2) a subsequent activity, dependent on an intact ATPase domain, which is required for extension of the incoming strand by DNA polymerases.

Yeast (12, 13) and *Drosophila* (26) Rad54p are able to use the energy derived from ATP hydrolysis to enhance the accessibility of nucleosomal DNA *in vitro*. Furthermore, Rad54p is required for Rad51-dependent strand invasion *in vitro* on nucleosomal donors (12). *In vivo*, Rad54p may hydrolyze ATP to remodel nucleosomes during the formation of stable recombination joints. Indeed, a positioned nucleosome occludes the HO recognition site at the *HML* donor locus (27), and this nucleosome may represent a barrier to DNA strand invasion or subsequent strand extension. To test for possible *in vivo* chromatin remodeling activity of Rad54p, MNase digestion of formaldehyde cross-linked chromatin was used to probe for changes in nucleosome positions at *HML* during strand invasion. However, we were not able to detect significant changes in the MNase digestion pattern even in the wild-type *RAD54* strain (data not shown). The exception was the appearance of a hypersensitive site that mapped to the HO recognition site at *HMLα*. Surprisingly, this DNA cleavage is due to the HO endonuclease. The cleavage is observed in the absence of MNase addition but requires galactose induction of HO (Fig. 5*b*, compare *lanes 1* and *5* with galactose with *lanes 4* and *8*, respectively, without galactose). Increasing the duration of galactose induction leads to greater amounts of cleavage at this site (data not shown). Detection of this cleavage product does not require extended periods of HO expression as a 30-min pulse of galactose, followed by glucose repression, still leads to 10–15% cleavage of *HMLα*.

To investigate whether the HO recognition site at *HML* becomes accessible as a consequence of DNA strand invasion, we performed the analysis in the isogenic *RAD54*, *rad54K341A*, and *rad54* deletion strains. Strikingly, the HO cleavage at *HML* does not occur in the *rad54* deletion strain or in the strain that expresses the ATPase-defective version, rad54K341A (Fig. 5*B*, compare *lanes 1* and *5* with *lanes 2* and *6*). Thus, these data indicate that accessibility of the HO site at *HML* requires a successful strand invasion event, and it is not due simply to overexpression of HO. Furthermore, since successful homology search and synapsis occur in the rad54K341R mutant (Fig. 4*b*), the induced accessibility at the *HML* HO site reflects a subsequent *RAD54*-dependent step. Accessibility may be a direct consequence of the ATP-dependent chromatin remodeling activity of Rad54p, or alternatively, it may require a later step in HR, such as DNA polymerase-dependent extension of the incoming DNA.

To directly address a possible involvement of DNA polymer-

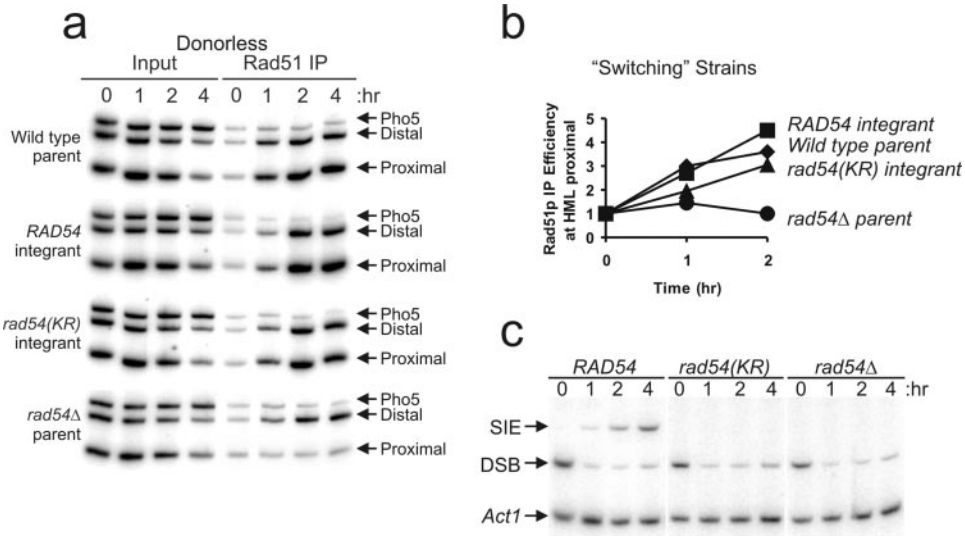

FIG. 4. **Rad54 mediator activity does not require an intact ATPase domain.** *a*, rescue of Rad54 mediator activity at *MAT* in donorless strains. A *rad54*Δ strain was transformed with an integrating vector containing either wild-type *RAD54* or the ATPase-defective *rad54K341R* allele. The wild-type donorless strain is included as a control. PCR products are indicated as in Fig. 1*b*. *b*, rescue of Rad54 mediator activity in strains harboring homologous donors. ChIP assays were performed as in *panel a* using the *HML*-proximal primer pair (Fig. 3*a*). IP efficiency was determined as in Fig. 1. *c*, extension of the invading strand from the *MAT* locus (SIE) requires ATPase activity of Rad54p. Input DNA from the ChIP assays in *panel b* were tested with primers for the appearance of the DSB and SIE product.

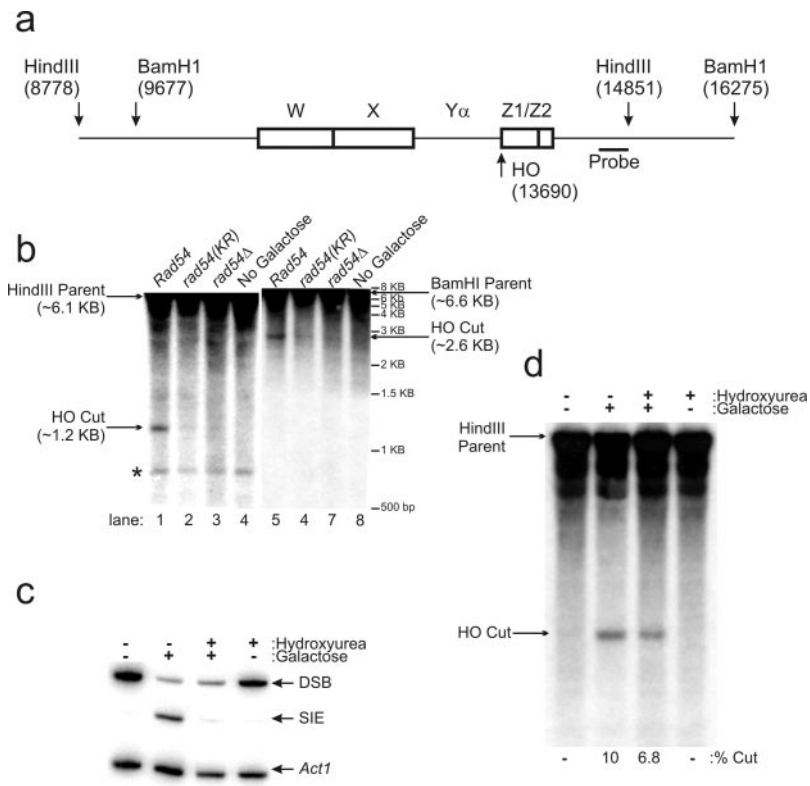

FIG. 5. **Rad54 remodels a nucleosome at *HML*.** *a*, schematic diagram of the *HML* locus indicating locations of the relevant restriction sites, HO recognition site, and Southern blot probe. *Numerical coordinates* represent the distance from the left-arm telomere of chromosome 3 in base pairs. *b*, representative gel demonstrating the appearance of HO cleavage at *HML*. Genomic DNA purified from yeast after galactose (30 min followed by 90 min of glucose) induction of HO was digested with either HindIII (*lanes 1–4*) or BamHI (*lanes 5–8*). The bands representing genomic DNA cut solely by the restriction enzymes (*Parent*) are indicated as are the bands resulting from further cleavage by HO (*HO Cut*). The *asterisk* indicates a nonspecific band that appears in some experiments. *c*, treatment with hydroxyurea blocks extension of the invading strand (SIE) in a wild-type *RAD54* strain but does not interfere with DSB induction. Cells were treated with hydroxyurea until they had arrested in S-phase. A fraction of the DNA used in *panel d* was tested for DSB induction and SIE. *d*, hydroxyurea treatment does not significantly reduce the HO sensitivity at *HML* in a wild-type *RAD54* strain. The DNA used here was the same as in *panel c*.

ase activity in the enhanced accessibility of *HML* donor chromatin, we treated yeast with hydroxyurea for several hours to deplete nucleotide pools, block DNA polymerase activity, and arrest cells in early S phase. Galactose was then added to the arrested cells to induce the formation of the DSB at *MAT*. As shown in Fig. 5*c*, hydroxyurea treatment has no effect on the efficiency of DSB formation at the *MAT* locus, but hydroxyurea did abolish the formation of a 30-bp strand invasion/extension product at *HML*. Notably, hydroxyurea treatment had only a minor effect (~30% decrease) on the HO cleavage at *HML* (Fig. 5*d*). Thus, the increased accessibility of *HML* chromatin does not require extension of the DNA strand by DNA polymerases, but the enhanced accessibility to HO appears to reflect a *RAD54*-dependent step that occurs after completion of a successful homology search. These data are consistent with a model in which the nucleosome that is positioned over the HO cleavage site inhibits the formation of the completely intertwined DNA joint, and ATP-dependent chromatin remodeling by Rad54p overcomes this barrier, facilitating the formation of a stable DNA joint that can be extended by DNA polymerases.

DISCUSSION

We have previously demonstrated that Rad54p has chromatin remodeling activity *in vitro* (12). Here, we present the first

evidence that Rad54 protein remodels chromatin *in vivo*. In this case, Rad54p requires an intact ATPase domain to remodel at least one nucleosome positioned over the HO cleavage site at the *HML* donor locus. *In vitro*, the ATP-dependent remodeling activity of Rad54p leads to enhanced accessibility of nucleosomal sites to restriction enzymes, but it does not appear to lead to dramatic changes in the positioning of nucleosomes within array substrates (12). Likewise, *in vivo*, we were unable to detect significant changes in nucleosome positioning by MNase analysis during the early stages of strand invasion, even when chromatin states were fixed with formaldehyde. Thus, the data are consistent with the idea that ATP-dependent remodeling by Rad54 may lead to enhanced accessibility of nucleosomal DNA without large scale nucleosome movements.

Previous studies have suggested that Rad54p has both ATP-dependent and -independent functions *in vivo* (1, 21, 24, 28). Here, we have confirmed these observations and identified the functions. The presynaptic activity of Rad54p does not require an intact ATPase domain, and consequently, a sonication-sensitive DNA joint is formed at a donor locus in the presence of an ATPase-defective version of Rad54p. The ATP-dependent activity of Rad54p appears to comprise, at least in part, an ATP-dependent chromatin remodeling function that facilitates the formation of a stable DNA joint that can be acted on by DNA polymerases. Whether there exist additional ATP-dependent steps for Rad54p remains to be investigated. The dual functionality of Rad54p may have evolved as genomes became larger and more highly condensed chromatin structures began to interfere with HR. A mutation that disrupts the ATPase domain of human *RAD54* is found in some tumors (29), suggesting that ATP-dependent chromatin remodeling by Rad54 may play a key role in maintaining genome integrity among all eukaryotes.

Acknowledgments—We thank Jim Haber for providing yeast strains, Hannah Klein for the *RAD54* plasmid, and Manolis Papamichos-Chronakis for assistance in developing the formaldehyde cross-linking micrococcal nuclease assay.

REFERENCES

1. Kim, P. M., Paffett, K. S., Solinger, J. A., Heyer, W. D., and Nickoloff, J. A. (2002) *Nucleic Acids Res.* **30,** 2727–2735
2. Pāques, F., and Haber, J. E. (1999) *Microbiol. Mol. Biol. Rev.* **63,** 349–404
3. Cromie, G. A., Connelly, J. C., and Leach, D. R. (2001) *Mol. Cell* **8,** 1163–1174
4. Sung, P., Trujillo, K. M., and Van Komen, S. (2000) *Mutat. Res.* **451,** 257–275
5. Haber, J. E. (1998) *Annu. Rev. Genet.* **32,** 561–599
6. Sung, P. (1997) *J. Biol. Chem.* **272,** 28194–28197
7. Wolner, B., van Komen, S., Sung, P., and Peterson, C. L. (2003) *Mol. Cell* **12,** 221–232
8. Sung, P. (1997) *Genes Dev.* **11,** 1111–1121
9. Sugawara, N., Wang, X., and Haber, J. E. (2003) *Mol. Cell* **12,** 209–219
10. Petukhova, G., Sung, P., and Klein, H. (2000) *Genes Dev.* **14,** 2206–2215
11. Eisen, J. A., Sweder, K. S., and Hanawalt, P. C. (1995) *Nucleic Acids Res.* **23,** 2715–2723
12. Jaskelioff, M., Van Komen, S., Krebs, J. E., Sung, P., and Peterson, C. L. (2003) *J. Biol. Chem.* **278,** 9212–9218
13. Alexeev, A., Mazin, A., and Kowalczykowski, S. C. (2003) *Nat. Struct. Biol.* **10,** 182–186
14. Alexiadis, V., and Kadonaga, J. T. (2002) *Genes Dev.* **16,** 2767–2771
15. Clever, B., Interthal, H., Schmuckli-Maurer, J., King, J., Sigrist, M., and Heyer, W. D. (1997) *EMBO J.* **16,** 2535–2544
16. Golub, E. I., Kovalenko, O. V., Gupta, R. C., Ward, D. C., and Radding, C. M. (1997) *Nucleic Acids Res.* **25,** 4106–4110
17. Petukhova, G., Stratton, S., and Sung, P. (1998) *Nature* **393,** 91–94
18. Solinger, J. A., and Heyer, W. D. (2001) *Proc. Natl. Acad. Sci. U. S. A.* **98,** 8447–8453
19. Mazin, A. V., Bornarth, C. J., Solinger, J. A., Heyer, W. D., and Kowalczykowski, S. C. (2000) *Mol. Cell* **6,** 583–592
20. Mazin, A. V., Alexeev, A. A., and Kowalczykowski, S. C. (2003) *J. Biol. Chem.* **278,** 14029–14036
21. Petukhova, G., Van Komen, S., Vergano, S., Klein, H., and Sung, P. (1999) *J. Biol. Chem.* **274,** 29453–29462
22. Church, G. M., and Gilbert, W. (1984) *Proc. Natl. Acad. Sci. U. S. A.* **81,** 1991–1995
23. Tan, T. L., Essers, J., Citterio, E., Swagemakers, S. M., de Wit, J., Benson, F. E., Hoeijmakers, J. H., and Kanaar, R. (1999) *Curr. Biol.* **9,** 325–328
24. Solinger, J. A., Kiianitsa, K., and Heyer, W. D. (2002) *Mol. Cell* **10,** 1175–1188
25. Peterson, C. L. (1996) *Curr. Opin. Genet. Dev.* **6,** 171–175
26. Alexiadis, V., Lusser, A., and Kadonaga, J. T. (2004) *J. Biol. Chem.* **279,** 27824–27829
27. Weiss, K., and Simpson, R. T. (1998) *Mol. Cell. Biol.* **18,** 5392–5403
28. Swagemakers, S. M., Essers, J., de Wit, J., Hoeijmakers, J. H., and Kanaar, R. (1998) *J. Biol. Chem.* **273,** 28292–28297
29. Smirnova, M., Van Komen, S., Sung, P., and Klein, H. L. (2004) *J. Biol. Chem.* **279,** 24081–24088

ATP-dependent and ATP-independent Roles for the Rad54 Chromatin Remodeling Enzyme during Recombinational Repair of a DNA Double Strand Break

Branden Wolner and Craig L. Peterson

J. Biol. Chem. 2005, 280:10855-10860.
doi: 10.1074/jbc.M414388200 originally published online January 14, 2005